Macromolecular Research, Vol. 23, No. 12, pp 1103-1111 (2015)
DOI 10.1007/s13233-015-3146-6

www.springer.com/13233
pISSN 1598-5032 eISSN 2092-7673

The Effects of Structure of Inclusion Complex between β-Cyclodextrin and Poly(L-lactic acid) on Its Performance

YuFang Zhou, YaNan Song, WeiJun Zhen*, and WenTao Wang

Key Laboratory of Oil and Gas Fine Chemicals, Ministry of Education and Xinjiang Uygur Autonomous Region, Xinjiang University, Urumqi 830046, P. R. China

Received April 19, 2015; Revised July 29, 2015; Accepted August 26, 2015

Abstract: The partial inclusion complexes (ICs) between poly(L-lactic acid) (PLLA) with high molecular weight and β-cyclodextrin (CD) were prepared and characterized by ^{1}H nuclear magnetic resonance spectra (^{1}H NMR), X-ray diffraction (XRD), thermogravimetric analysis (TGA), differential scanning calorimetry (DSC) and polarizing optical microscopy (POM), respectively. The thermal results demonstrated that the crystallization performance of ICs were significantly improved, and the decomposition temperature of ICs were increased compared with PLLA. The mechanical tests indicated that the mechanical performance of ICs was improved, and the β-CD-PLLA ICs exhibited a higher non-Newtonian effect than PLLA. The degradation rate for the partial ICs in phosphate buffer solution accelerated as the ratio of β-CD increased, meanwhile, the partial ICs had a good shape memory behavior. The wetting measurements suggested the hydrophilicity of ICs was also enhanced markedly in comparison with the bulk PLLA.

Keywords: β-cyclodextrin, poly(L-lactic acid), inclusion complex, performance.

Introduction

Cyclodextrins (CD) are a series of cyclic oligosaccharides consisting of more than six D (+)-glucose units joined by α-1,4-linkages. According to the number of glucose unit in CD macrocycles, from six to eight, the molecules are termed as α-, β-, and γ-CD, respectively. The unique structure, like a truncated cone including a hydrophilic outer surface and hydrophobic cavity, has the capacity to accommodate different guest molecules.[1-4] The formation of host-guest inclusion compounds shows the importance in both designing and constructing the nanometer-scale ordered structures.[5] In recent years, due to potential applications in many areas, much attention has been given to the formation between linear polymeric guests and CDs leading to the main chain pseudopolyrotaxanes by several groups.[5-7]

As a synthetic biodegradable polyester, poly(L-latic acid) (PLLA) have been of special interest in biomaterials such as scaffolds engineering,[8-12] surgical suture[13] and shape memory polymers (SMP)[14] depending on its favourable chemical, biological and mechanical characteristics including structural simplicity and compatibility. However, these defects such as poor wettability, brittleness, bad impact resistence and thermal stability, severely restrict its potential application in other aspects.[8-14] It was worth noting that the introduction of good water-soluble cyclodextrins threaded on polymer chains could not only improve the hydrophilcity of polymer surfaces, but also show some effect on its crystallization, degradation and thermal stability performances, resulting from these facts that the hydrophobic cavities would restrict the motion of macromolecular chains and increase the degree of crosslinking.[15-18] To our best knowledge, there were some reports about the inclusion complexes between poly(lactic acid) (PLA) and cyclodextrins, for instance Oliveira *et al.*[19] discovered that α-cyclodextrin could form inclusion structures with poly(D,L-lactic acid) (PDLLA), and bulk PDLLA presented a typical Vogel-Fulcher-Tammann-Hesse (VFTH) behavior while the ICs dynamics showed an Arrhenius trend; Zhang[20] also prepared the α-CD-PLA ICs and found that the presence of PLA-IC significantly promoted the crystallization of PLA; Xie *et al.*[21] similarly reported that glass transition temperature (T_g) value of ICs between PLA with high molecular weight and β-CD decreased compared with PLA, furthermore, β-CD-PLLA ICs had improved hydrophilicity, but the in-depth effects on the structure and other properties of β-CD-PLLA ICs were not investigated. In viewing the modification of PLA materials through inclusion complex with cyclodextrin, it was very necessary to investigate the effect of inclusion structure on the performance of PLA. Meanwhile, the influences of the mole inclusion ratios between cyclodextrin and other polymers on their performances, such as thermal behavior[22,23] surface properties[24] and so on, were also mentioned briefly in the previous

*Corresponding Author. E-mail: zhenweijun6900@163.com

work, but the systematic studies and how the supramolecular structures of ICs with various stoichiometric ratios affect the performances of the PLA polymer were rarely mentioned.

On the basis of these considerations, the partial *β*-CD-PLLA inclusion compounds with different stoichiometric ratios were obtained by co-precipitation method in this work; then the crystallization performance and mechanical properties of the two partial ICs were studied by differential scanning calorimetry (DSC), polarized optical microscopy (POM), dynamic mechanical analysis (DMA), and tensile measurements. Then the potential relationships between the supramolecular structures and the performances of the partial ICs were studied. In addition, according to the proposed structures and the differences of crystallization between the uncovered polymer chain and the parts covered by cyclodextrin cavities in partial ICs, their shape memory behaviors were investigated and testified through theoretical proof, *i.e*., the modulus variation around T_g, $E_{Tg+20\,^oC}/E_{Tg-20^oC}$. As it is well known, it is the slow degradation behavior of bulk PLA polymer with high molecular weight would bring some difficulty in recovery and reprocessing for polymer composite materials, and thus the degradation speed also became an important indicators for evaluation of the polymer materials. In order to elaborate the effects of *β*-CD host-guest inclusion interactions on the degradation of PLLA, the degradation behaviors in phosphate buffer solution (PBS) of the two partial ICs with different inclusion ratios were investigated.

Experimental

Materials. The injection grade PLLA (the weight-average molecular weight was 1×10^5 g mol^{-1}) used in the work was obtained from Shengzhen Guanghua weiye Industrial Co. (China); *β*-cyclodextrin, analytically pure, was purchased from Tianjin Guangfu Fine Chemical Industry Research Institute (China); Disodium hydrogen phosphate, sodium dihydrogen phosphate, analytically pure, were obtained from Tianjin Kemeng Chemical industry & trade Co., LTD (China); Normal analytical pure chloroform, *N*,*N*-dimethylformamide and sodium chloride were used without further purification.

Preparation of the *β*-CD-PLLA Inclusion Complexes. A general procedure of preparation of *β*-CD inclusion complexes with PLLA (*β*-CD-PLLA ICs) was as follows: PLLA were dissolved in chloroform, and then PLLA solution was dropwise added into the *β*-CD saturated aqueous solution with strongly stirring at room temperature for predetermined intervals, and the mixture turned turbid. Then the solution was allowed to stand for 48 h. The precipitate was collected by filtration and washed by $CHCl_3$ and distilled water three times to remove uncovered PLA and free *β*-CD, respectively. The products were dried in vaccum oven at 50 °C for 48 h.

Shape Memory Behavior Test. 1.5 g of the *β*-CD-PLLA IC1 was dissolved in 50 mL of dimethylformamide (DMF) at 60 °C, after initial stirring for 2 h, then the solution was poured into a glass dish slowly; in order to remove the solvent thoroughly, the glass dish was put in the fume hood for 48 h; finally the film was placed in a vacuum drying oven at 50 °C for 48 h. Following this, the film was cut into several straight strips (3.5×0.5×0.01 cm) to test the shape memory behavior. According to the testing method reported by Luo *et al*.,[25] the straight strip of ICs was deformed to an angle θ_o=90° at 100 °C under external force and then cooled down to room temperature to maintain the deformation θ_i. The deformed sample was rapidly heated again to 95 °C and the deformation angle θ_d was recorded. The recovery ratio was defined as $(\theta_i-\theta_d)/\theta_i$. The fixity ratio was defined as θ_i/θ_o. The recovery time is the time required for the deformed shape to recover its original shape.

***In vitro* Degradation.** The PBS was prepared with 0.2 g NaH_2PO_4, 2.2 g Na_2HPO_4 and 8.5 g NaCl, and then the specimens were immersed into 800 mL of the buffer solution with pH=7.4 in a incubator at 37 °C. The sampling operation was performed every few days and the samples were washed by distilled water three times to remove residual phosphate, and dried to a constant weight in a vaccum at 50 °C for 48 h. Meanwhile, the buffer solution needed to be changed regularly to keep a constant pH value. The specimens were weighed before and after degration, marked as W_0, W_i respectively, the mass retention ratio was caculated by this equation: $M_i=(W_i/W_0)\times100\%$.

Measurements.

^{1}H NMR: ^{1}H NMR spectra were recorded on INOVA 400 MHz spectrometer (VARIAN, Co., LTD, USA) in the solvent DMSO-d6 at room temperature.

XRD: X-Ray diffraction (XRD) patterns were recorded with X-ray diffractometer (Philips X'Pert, Netherland), using CuK_α X-ray source at λ=0.1540 nm (50 Kv, 35 mA). Diffraction spectra were obtained over 2θ range of 5°-40° with a step interval of 0.1°/s. Samples were operated from the injection mold. Before testing, the samples were dried to a constant weight at 55 °C in a vacuum oven.

TGA: Thermogravimetric analysis (TGA) was conducted on TA Q600 thermal-gravimetric analyzer (USA). 5 mg of samples were performed by heating from room temperature to 700 °C at a heating speed of 10 °C/min on the condition of a nitrogen flow.

DSC: Differential scanning calorimetry (DSC) measurements were performed with NETZSH differential scanning calorimeter (DSC-204, Germany). In order to detect the glass transition clearly, samples of 6 mg were performed by heating from room temperature to 220 °C at a heating rate of 5 °C/min, after erasing the thermal history at 220 °C within 5 min, then cooled down to 20 °C at 5 °C/min under a nitrogen flow.

DMA: Dynamic mechanical analysis (DMA) was performed using a DMA Q800 V7.5 instrument in the strain mode at a fixed frequency of 1Hz and nitrogen gas purging. The measured specimens were heated from 30 to 140 °C.

Tensile Measurements: The tensile tests were conducted by a Universal Testing Machine (Instron 4302, USA) accord-

ing to ASTM D412-80 at a crosshead speed of 50 mm/min. The samples were injection molded and dried at 60 °C in vacuum oven for 24 h.

Rheological Properties: The rheological performance was investigated by a Bohlin Gemini 200 instrument (Marlven, Britain). The samples were molded into several wafers (the diameter was 25 mm and thickness was 1 mm) by hot-pressing. The temperature went up to 200 °C with a speed of 3 °C/min, stood for a few minutes until the wafers were completely melted, then colded down to 25 °C at a speed of 3 °C/min under the nitrogen flow. The complex/storage modulus curves over frequency were recorded under different period of time.

POM Measurements: The spherulitic morphologies of the samples were investigated on a Nikon FE Fil (Japan) polarizing microscope, equipped with a digital camera system and a Linkam THMS 600hot stage. The samples were heated to 200 °C, and then stood for 5 min at the constant temperature, cooled down to 120 °C quickly for isothermal crystallization. To observe the spherulite growth rate, the pictures were taken at different period of time in the crystallization process.

The Wetting Performance: Static contact angle of water on the ICs surface was determined by a contact angle meter (JJ2000B2, Zhongchen Digital Technology Co., China). The specimen was pressed into small sheets with the 2 mm thickness by a SSP-10 type tablet press before testing.

Results and Discussion

The Structures Characterization of the β-CD-PLLA ICs. The ^{1}H nuclear magnetic resonance (NMR) spectra of β-CD-PLLA inclusion complexes compared with PLA and β-CD were illustrated in Figure 1; in view of the ICs, the characteristic resonances for PLLA and β-CD were clearly discovered from Figure 1(c) and (d), The host-guest stoichiometry (*i.e.* CD: PLLA, mol: mol) of ICs could be calculated by the integration of NMR resonances belonging to CD blocks at 4.83 ppm and to PLLA blocks at 1.5 ppm. The actual content of CD in the β-CD-PLLA inclusion complexes were given in Table I, respectively. The small molar inclusion ratios between CD and PLLA with high molecular weight indicated the strong steric hindrance effects of polymer chain would be unfavorable for the inclusion formation significantly.

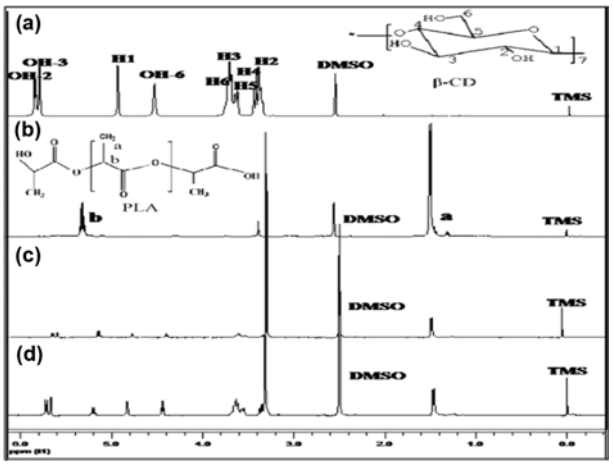

Figure 1. ^{1}H NMR patterns of (a) β-CD, (b) PLLA, (c) β-CD-PLLA IC1, and (d) β-CD-PLLA IC2.

Table I. The Encapsulation Ratios of CD in the β-CD-PLLA ICs Calculated by ^{1}H NMR

Samples	Mole Ratio of Monomer: CD (mol:mol)	Mass Content of CD in ICs (wt%)[a]
PLLA	-	0
β-CD-PLLA IC1	1:0.07	53.47
β-CD-PLLA IC2	1:0.18	73.94

[a]The mass content of CD in ICs was calculated by the formula: W % $=1135\times n_a/(1135\times n_a+72\times(1-n_a))$, in which the molar molecular weight for β-CD and the repeated unit was 1135 and 72 g mol^{-1}, respectively; n_a was the mole ratio for CD in ICs by ^{1}H NMR.

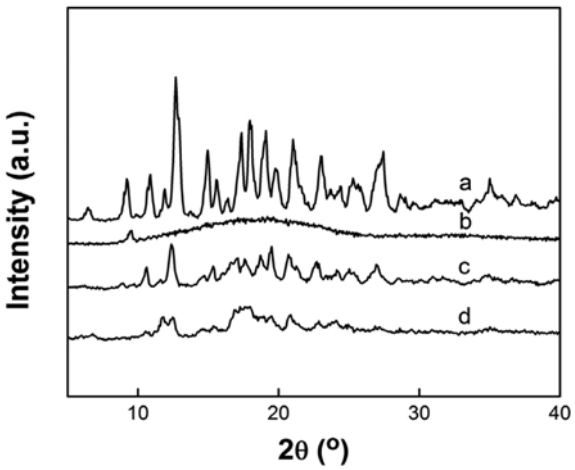

Figure 2. XRD patterns of (a) β-CD, (b) PLLA, (c) β-CD-PLLA IC1, and (d) β-CD-PLLA IC2.

The XRD patterns of β-CD, PLLA, β-CD-PLLA IC1 and β-CD-PLLA IC2 were shown in Figure 2, respectively. The major peaks at 2θ=12.5° and 22.5° were observed for pure β-CD, and the only wide diffraction peak attributable to PLLA was located at 2θ=15-22°.[26,27] However, it could be found that the XRD pattern of β-CD-PLLA ICs was not only totally different from that of pure PLLA and β-CD, but also not simple blends from Figure 2(c) and (d). It was indicated that the inclusion interaction between PLLA and β-CD had occurred.[28] Besides that, with the ratio of β-CD increasing, the intensities of characteristic peaks were weakened and the peak areas broaden in β-CD-PLLA IC2 compared to that of β-CD-PLLA IC1. This might be due to the facts that PLLA chains were partially included, so that the uncomplexed parts of polymer chains were still able to aggregate to form a crystalline phase coexisting with IC crystals,[29] which would have an important effect on the structure and properties of PLA after introduction of

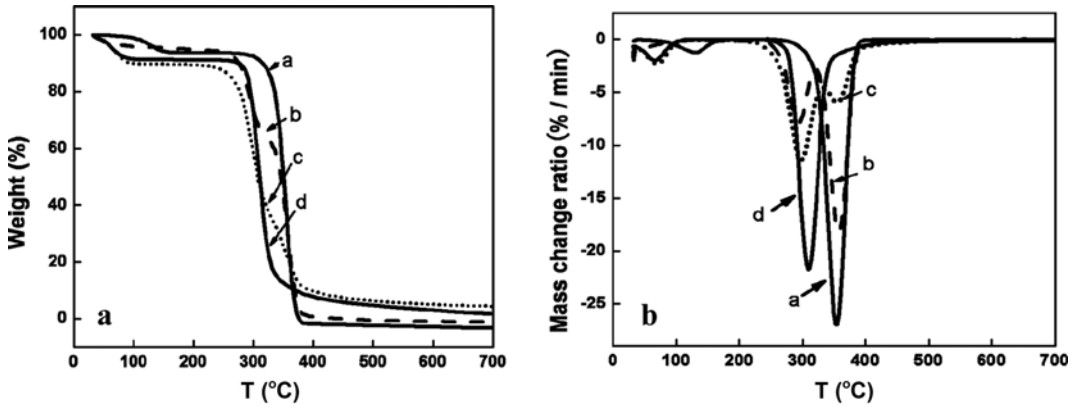

Figure 3. TG and DTG curves of (a) PLLA, (b) *β*-CD-PLLA IC1, (c) *β*-CD-PLLA IC2, and (d) *β*-CD.

β-CD in PLA chain.

The Thermal Properties of β-CD-PLLA ICs. According to TGA curves of the *β*-CD-PLLA ICs and pure PLLA in Figure 3(a) and (b), an increase of 3.8 °C in view of thermal decomposition temperature was obviously seen for the inclusion complexes compared to pure PLLA, and meanwhile, owing to more addition of *β*-CD cavities on the polymer chain, the peak value of the IC2 shifted to a higher thermal decomposition temperature than that of IC1; these results showed that after the introduction of *β*-CD on the polymer chains, the thermal stability of PLLA had been improved to a certain extent and the partial IC2 showed a better thermal behavior. Similar results also had been reported in the literatures.[30-32] Meanwhile, from the thermogravimetry (TG) and derivative thermogravimetry (DTG) curves (Figure 3(a) and (b)), it was found that the decomposition of ICs would undergo a two-step process, in which it started to decompose at the decomposition temperature (T_d=293.6 °C) assigned to *β*-CD, and then another thermal decomposition peak occurred at T_d=357.4 °C for the PLLA segments in ICs. Depending on TGA curves, the decomposition temperature of samples was listed in Table II. The content of *β*-CD in ICs was also estimated roughly, namely 37.4 and 69.1 wt%, respectively, which were nearly consistent with the results by ^{1}H NMR.

From DSC measurements of the *β*-CD-PLLA ICs in Figure 4, it could been observed that there was a strong and broadened melting peak at 149.8 °C for the partial ICs compared to that of pure PLLA at 148.1 °C within the heating scans. The crystallization degree of PLLA segments in the ICs could be calculated by the formula: $X_c=(\Delta H_m/\Delta H_O)\times 100\%$, X_c was the crystallization degree of composites, ΔH_m respresents the melting enthalpy of composite materials, and ΔH_O was the melting enthalpy of PLLA with complete crystallization, namely 93.7 J g^{-1} [33] (Table III). The results indicated that the crystallization performances of ICs were significantly enhanced compared with PLLA, and the partial IC2 revealed a better crystallization behavior up to 10.28% compared with the crystallization degree (X_c=9.86%) of IC1. Meanwhile, the findings of ICs from DSC curves were also different from the ICs with a column structure reported in the previous work.[34,35] The explanation might be that PLLA with high molecular weight merely formed a partial inclusion structure with cyclodextrin, and it was attributable to the limited mobility of uncovered part of polymer segments constrained by its included part residing in the *β*-CD cavity, leading to the acceleration of PLLA crystallization.

Table II. The Decomposition Temperature and CD Content of the *β*-CD-PLLA ICs Determined by TGA

Samples	T_d (°C)	CD Content (wt%)
PLA	354.8	-
β-CD	308.3	100
β-CD-PLA IC1	357.4	37.4
β-CD-PLA IC2	358.6	69.1

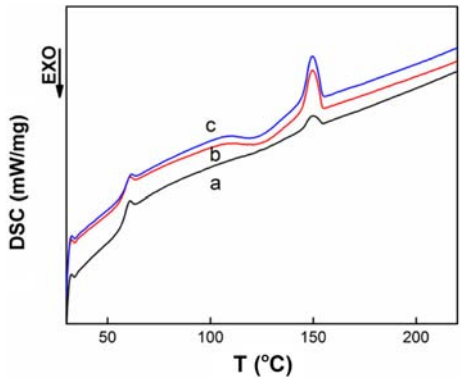

Figure 4. DSC curves of (a) PLA, (b) *β*-CD-PLLA IC1, and (c) *β*-CD-PLLA IC2.

Table III. The Crystallization Parameters of the *β*-CD-PLLA ICs Calculated by DSC

Samples	T_m (°C)	ΔH_m (J/g)	X_c (%)
PLLA	148.1	2.42	2.58
β-CD-PLLA IC1	149.5	9.24	9.86
β-CD-PLLA IC2	149.8	9.64	10.28

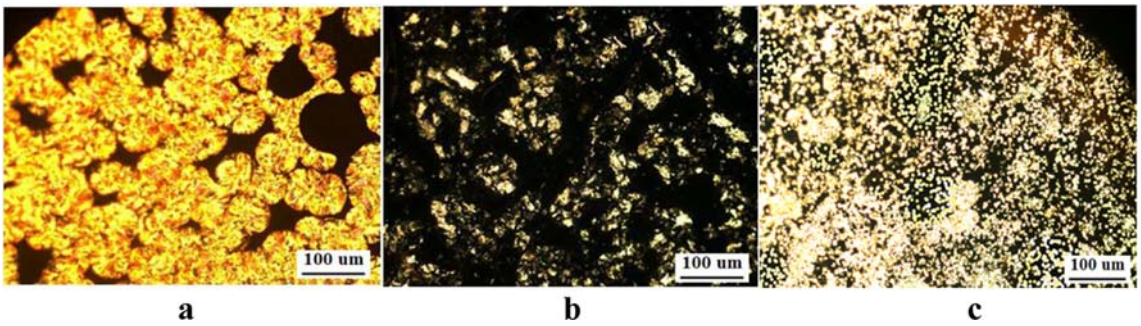

Figure 5. The POM images of (a) PLLA, (b) *β*-CD-PLLA IC1, and (c) *β*-CD-PLLA IC2 at the 10 min during crystallization process.

Spherulitic Morphology of the *β*-CD-PLLA ICs. The polarized optical microscopy (POM) was used to record the growth speed and size of the spherulites of PLA. Figure 5 showed the grain morphologies of pure PLLA and *β*-CD-PLLA ICs crystallized at 120 °C after quenched directly from 200 °C within different periods. It could be observed clearly that the diameter of pure PLLA spherical grains reached up to 100 μm. However, after PLLA formed an inclusion structure with *β*-CD cavities, the crystallization speed of all the ICs accelerated and the sizes of IC2 grains began to become smaller and the surface morphology also turned irregular, but the nucleation density increased significantly compared with PLLA and IC1. POM analysis further confirmed that inclusion structures of PLLA had more prominent efficiency on inducing the crystallization of PLLA, which were also in good accordance with the DSC results.

As it is well known, two main mechanisms, namely chemical nucleation and epitaxial nucleation have been widely accepted to elucidate the nature of nucleation phenomena of nucleating agent addition in polymers.[36] As regards the chemical nucleation, the nucleating agent dissolves in the polymer melts and reacts with it, leading to the scission of polymer chains and the formation of ionic end groups which constitute the true nucleating species.[37] In our work, POM observation found that *β*-CD did not dissolve in the molten PLLA. Furthermore, *β*-CD was not able to react with PLLA chains, which indicated that chain scission of PLLA was not able to be caused by chemical reaction happening during the inclusion process between PLLA and *β*-CD. Consequently, the nucleation mechanism of PLLA induced by the chemical mechanism between PLLA and *β*-CD was eliminated. In view of epitaxial nucleation, the polymer chains epitaxially grow on the surface of nucleating agent substrate through a physical interaction, and what is more, a good lattice matching between the two crystal structures of polymer and nucleating agent does matter.[38-41] As regarding to our work, the hydrogen bond interaction between PLLA and *β*-CD might play an important role in the nucleation process. However, additional information is still needed for an in-depth investigation of the exact nucleation mechanism.

Mechanical Performance of the *β*-CD-PLLA ICs. As known, from the DMA curves, we could know some information about the mobility of polymer segments in ICs and measure the T_g of polymers. Besides that, more information about the storage modulus, loss modulus and damping behavior could be obtained. As illustrated in Figure 6(a) and (b), the curves of the storage modulus and tanδ as a function of temperature of pure PLLA and *β*-CD-PLLA ICs were given, respectively. All the storage modulus curves exhibited a decreasing trend as temperature increased. And the values of PLLA were higher than that of ICs before the temperature went up to T_g, but the ICs showed a reverse trend after T_g of PLLA.

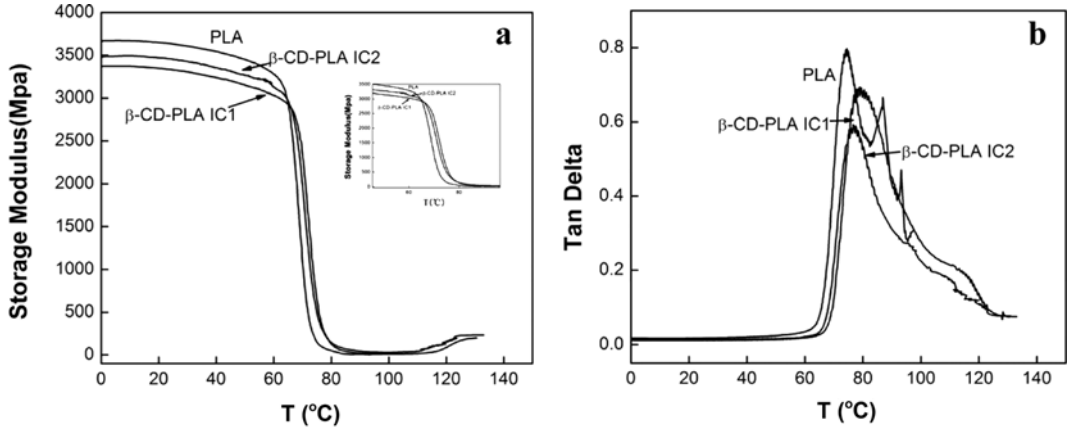

Figure 6. The dynamic mechanical analysis curves of *β*-CD-PLLA ICs.

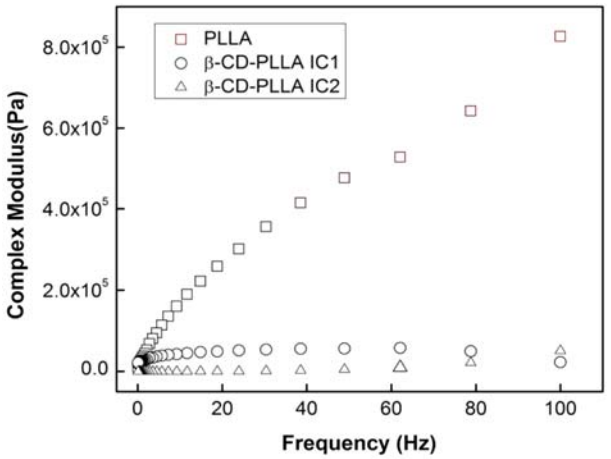

Figure 7. The rheological properties of *β*-CD-PLLA ICs and neat PLLA.

The partial IC2 with higher *β*-CD ratio had the smaller storage modulus compared to the IC1. These phenomenon might be explained by the facts that the *β*-CD -PLLA ICs showed a complete elastic behavior because of lower loss modulus before T_g, and while PLLA chains were encapsulated in CD cavities, the motility of PLLA chains were greatly constrained leading to the storage modulus decreasing quickly, and the behavior of the material began to change from a complete elastic state to viscous flow state as the temperature increased beyond T_g. From the curves of tanδ as the temperature, with the reducing storage modulus, the sharp peaks of loss modulus for the ICs and neat PLLA occurred around the glass transition temperature, and meanwhile, the T_g was estimated as 74.6 and 79.0 ºC for PLLA and IC1, respectively, an 4.4 ºC increase of T_g for the inclusion complex as compared with the bulk was found, which was also similarly reported by Viciosa.[42] The DMA results also evidenced that the confinement effect imposed by *β*-CD rings highly restricted the conformational dynamics of the PLLA chains in the ICs in agreement with the DSC results.

The rheological properties of *β*-CD-PLLA ICs and PLLA were showed in Figure 7. From the curves of complex modulus, the *β*-CD-PLLA ICs exhibited a higher non-Newtonian effect than PLLA, and a remarkable effect of frequency on the complex modulus was observed. As the frequency increased gradually, the complex modulus curve of pure PLLA was significantly improved while the ICs showed a reverse trend down the curve of polymer; the curve of IC2 was always located below that of IC1. The lower complex modulus values of ICs might be associated with the molecular chain entanglement in composite materials. Owing to the introduction of more *β*-CD cavities on the polymer chains, the entanglement effects were enhanced significantly, thus leading to a decreasing elasticity of the composite materials.

Figure 8 showed the tensile strength and elongation at break values of *β*-CD-PLLA ICs and PLLA. It could be observed that the tensile strength value of ICs decreased markedly from 51.8 to 42.68 MPa compared to that of PLLA with the ratio of *β*-CD increasing in the ICs. Meanwhile, the elongation at beak of ICs also had a similar variation trend, but the value of IC2 was slightly higher than IC1. These results manifested that the host-guest interactions between *β*-CD and PLLA and hydrogen bond effects reduced the intermolecular interaction force of PLLA, and led to its extension of relaxed process, thus changed the flexibility of PLLA segments. On the other hand, the partial *β*-CD-PLLA IC still contained some amount of *β*-CD, consequently, the interfacial interaction between the PLLA matrix and the *β*-CD was damaged by the hydrophilic *β*-CD, which resulted in the discontinuous PLLA matrix, so the above factors were responsible for the decrease of the tensile strength and elongation at break of the *β*-CD-PLLA ICs.

Surface Properties of *β*-CD-PLLA ICs. As shown in Figure 9, in order to characterize the surface wettability and hydrophilic property of the materials, the static contact angles on the surface for the *β*-CD-PLLA ICs and neat PLLA were measured, separately. According to the contact angle values of the ICs listed in Table IV, a marketable decrease was observed compared to pure PLLA, and with the increasing content of CD in the partial ICs, the IC2 had a lower contact angle than that of IC1. It could be concluded that the complexes had a

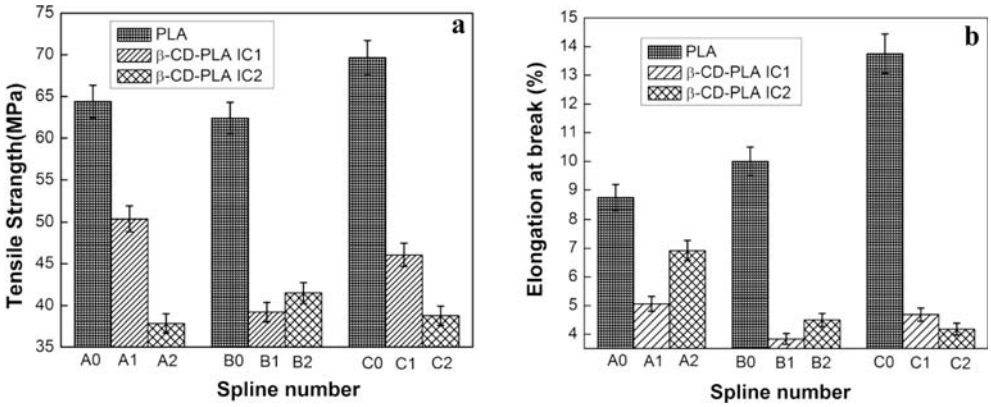

Figure 8. The tensile strength and elongation at break of *β*-CD-PLLA ICs and PLLA.

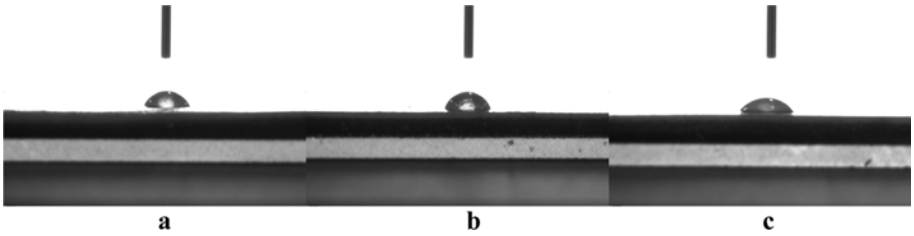

Figure 9. The contact angles of (a) PLLA, (b) β-CD-PLLA IC1, and β-CD-PLLA IC2.

Table IV. The Static Contact Angle Values for the β-CD-PLLA ICs with PLLA

Contact Angle (º)	Samples		
	PLLA	β-CD-PLA IC1	β-CD-PLA IC2
Theta(R) [deg]	71.1	66.7	52.0
Theta(L) [deg]	71.1	66.7	52.0
Theta(M) [deg]	71.1	66.7	52.0

higher hydrophilicity than PLLA and the different stoichiometric ratios of ICs would have a significant impact on surface properties of PLLA. The results might be ascribed to these facts that PLLA belongs to the polyester family, and lack of the hydrophilic functional groups in the chain structures tends to make PLLA a hydropholic surface; however, the cyclodextrin cavities containing a large number hydroxyl groups threading on the PLLA chain could improve interfacial compatibility between PLLA and other materials *i.e.* water molecules, leading to its surface from the hydropholic one to a hydrophilic one or the active surface translating into a inactive form due to reducing the surface active energy of PLLA during the information of inclusion complexes.

Shape Memory Behavior of the β-CD-PLLA ICs. In recent years, thermal responsive shape memory polymers had been of interest due to their attractive properties and potential applications in sensors, transducers and biomaterials.[43-45] As it is well known to us, the shape memory polymers (SMPs) should possess two separated phases: a fixing phase and a thermally reversible phase. The fixing phase with the higher phase transition temperature was responsible for the permanent shape, while the reversible phase had a lower T_{trans} and served as a thermal "switch" to fix the temporary shape under T_{trans}. In the study, the partial β-CD-PLLA ICs were used for shape memory testing in which the naked PLLA segment and the PLLA parts encapsulated by β-CD cavities accounted for the reversible phase and fixing phase, respectively. As demonstrated in Figure 10, the straight splines of the partial ICs were changed into a spiral shape at 100 ºC, and then cooled rapidly to room temperature in order to keep the deformation. When heated again to 95 ºC, the complex nearly recovered its original shape within 10 s. The recovery ratios and the variation of storage modulus above and below T_g for the β-CD-PLLA ICs were listed in Table V. The difference in storage modulus around T_g=75 ºC ($E_{Tg+20\,^oC}/E_{Tg-20\,^oC}$) was a significant property to describe the shape memory behavior of the partial inclusion compounds, a dramatic drop in the modulus (E) appeared for the ICs and the IC2 exhbited a higher modulus ratio and recovery ratio compared with IC1. The results demonstrated that the uncovered PLLA segments undergo through a large scale motion and the ICs became soft and flexible under heating above T_g, and the partial IC2 showed a good shape memory behavior consistent with its high storage modulus ratio.

***In vitro* Degradation Performance of β-CD-PLLA ICs.** The quality change was an important indicator to measure

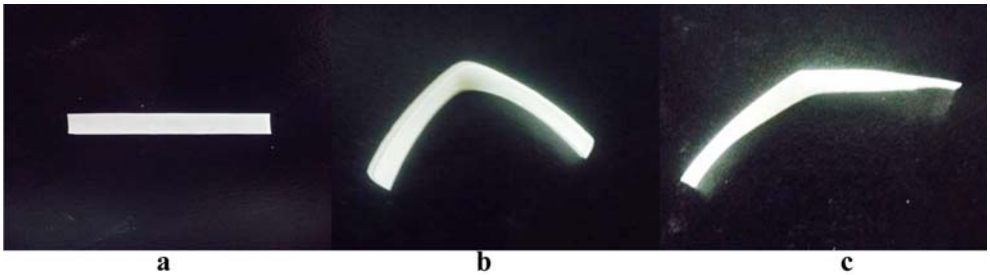

Figure 10. The images of the macroscopic shape memory behavior for the β-CD-PLLA IC2: (a) Original shape, (b) the deformed shape under external stress, and (c) the recovered shape obtained by heating to 95 ºC.

Table V. The Shape Memory Properties of β-CD-PLLA ICs

Samples	Fixing Ratios (%)	Recovery Ratios (%)	E_{Tg+20^oC} (MPa)	E_{Tg-20^oC} (MPa)	$E_{Tg+20^oC}/E_{Tg-20^oC}$
β-CD-PLLA IC1	91.0	80.5	3090.38	32.18	96.03
β-CD-PLLA IC2	93.5	88.8	3231.53	16.51	195.73

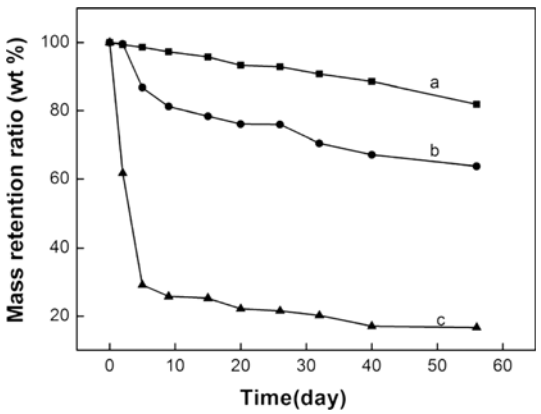

Figure 11. The curves of degradation from (a) bulk PLLA, (b) *β*-CD-PLLA IC1, and (c) *β*-CD-PLLA IC2.

the degradation situation for the samples. In this work, the *in vitro* degradation behaviors of the *β*-CD-PLLA ICs and neat PLLA were investigated in the phosphate buffer solution (PBS) with pH=7.4 at 37 ºC during two months, as illustrated in Figure 11. From the degradation curves of ICs with bulk PLLA, it was shown that the ICs had an obvious mass change during the whole process; in terms of PLLA, a weight retention of 98.2% had been monitored after 10 days, meanwhile the weight retention of *β*-CD-PLLA IC1 and *β*-CD-PLLA IC2 was 81.0% and 25.5%, respectively. The degradation of PLLA accelerated to a certain extent and the quality loss came to 20% in the 60 days.[46] It was worth noting that the weight retention of *β*-CD-PLLA ICs2 with more CD contents was higher than that of *β*-CD-PLLA IC1. The mass loss had been nearly more than 50% during the first week compared with 16% for the IC1, which means that the formation of the inclusion accelerated the degradation of PLLA. The results might be explained in two aspects: the formation of hydrogen bonds between hydroxyl groups contained in the cyclodextrins and H_2O in the phosphate buffer solution speeding up the hydrolytic process of polymer or the cyclodextrin rings gradually slided down from the PLA chain leading to the large mass loss of ICs during the degradation process.

Conclusions

The PLLA chains with high molecular weight possessed a stronger steric-hinerance effect and were not easily penetrated by *β*-CD cavities, thus the polymer chains tended to form the partial inclusion complexes with small stoichiometric ratios. However, it was this conformation difference between the polymer segments covered by CD cavites and the uncovered polymer chains that lead to the significant difference of crystallization performance for the ICs in comparison with bulk PLLA, in which the covered polymer segments by *β*-CD might play the role of nucleating agent and thus accelerate the crystallization of PLLA. Meanwhile, the decreasing storage modulus of the partial ICs compared with PLLA indicated that the polymer chain had gradually changed from the rigid state to an elastic state, which was also consistent with the results of the rheological measurements. Besides, the *β*-CD cavities with several hydroxyl groups could also enhance the surface hydrophilicity of PLLA markedly through decreasing intermolecular surface energy. The enormous difference in storage modulus around T_g of the partial IC2 allowed it with good shape memory behavior, which would provide some theoretical basis for PLLA composite materials in other applications. With the increasing ratio of CD, the IC2 exhibited a better degradation performance than bulk PLLA due to the difference in crystallization performance. The results also indicated the large effects of structures of the ICs on the properties of PLA, which could help us to understand the mechanism of the formation of inclusion complexation comprehensively.

Acknowledgments. We greatly appreciate that this work is financially supported by National Science Foundation of China (51263019).

References

(1) J. Li, B. Chen, X. Wang, and S. H. Goh, *Polymer*, **45**, 1777 (2004).
(2) Y. M. Zhang, X. R. Deng, L. C. Wang, and T. T. Wei, *J. Macromol. Sci. A: Pure Appl. Chem*., **45**, 289 (2008).
(3) M. A. Semsarzadeh and S. Amiri, *J. Incl. Phenom. Macrocycl. Chem*., **77**, 489 (2013).
(4) F. Zuo, C. Luo, X. Ding, Z. Zheng, X. Cheng, and Y. Peng, *Supramol. Chem.,* **20**, 559 (2008).
(5) J. Y. Li, D. Y. Yan, X. L. Jiang, and Q. Chen, *Polymer*, **43**, 2625 (2002).
(6) A. Harada, J. Li, and M. Kamachi, *Macromolecules*, **26**, 5698 (1993).
(7) I. G. Panova, V. I. Gerasimov, F. A. Kalashnikov, and I. N. Topchieva, *Polym. Sci. B*, **40**, 415 (1998).
(8) X. J. Wang, G. J. Song, T. Luo, and W. J. Peng, *J. Biomater. Sci.*, **20**, 1995 (2009).
(9) E. Díaz, I. Puerto, I. Sandonis, and I. Ibañez, *Polym. Plast. Technol. Eng.*, **53**, 150 (2014).
(10) S. I. Kim, B. R. Lee, I. L. Jin, and C. H. Mun, *Macromol. Res.*, **22**, 1229 (2014).
(11) J. H. Kim, T. K. Ryu, S. K. Moon, and J. S. Lee, *Macromol. Res.*, **23**, 501 (2015).
(12) M. Zhou, P. Zhou, P. Xiong, and X. Qian, *Macromol. Res.*, **23**, 231 (2015).
(13) S. Viju, G. Thilagavathi, and B. Gupta, *J. Text. I*, **101**, 835 (2010).
(14) J. Z. Liang, D. R. Duan, C. Tang, C. P. Tsui, and D. Z. Chen, *J. Macromol. Sci. B: Phys.*, **52**, 964 (2013).
(15) A. Harada, Y. Takashima, and M. Nakahata, *Chem. Res.*, **47**, 2128 (2014).
(16) B. V. K. J. Schmidt, M. Hetzer, H. Ritter, and C. Barner-Kowollik, *Prog. Polym. Sci.*, **39**, 235 (2014).

(17) T. Dong, W. H. Kai, P. J. Pan, A. Cao, and Y. Inoue, *Macromolecules*, **40**, 7244 (2007).
(18) K. Shin, T. Dong, Y. He, Y. Taguchi, A. Oishi, H. Nishida, and Y. Inoue, *Macromol. Biosci*., **4**, 75 (2004).
(19) T. Oliveira, G. Botelho, N. M. Alves, and J. F. Mano, *Colloid. Polym. Sci.*, **292**, 863 (2014).
(20) R. Zhang, Y. M. Wang, K. J. Wang, G. Q. Zheng, Q. Li, and C. Y. Shen, *Polym. Bull*., **70**, 195 (2013).
(21) D. M. Xie, K. S. Yang, and W. X. Sun, *Curr. Appl. Phys*., **7**, 15 (2007).
(22) B. R. Williamson and A. E. Tonelli, *J. Incl. Phenom. Macrocycl. Chem*., **72**, 71 (2012).
(23) N. Marangoci, A. Farcas, M. Pinteala, V. Harabagiu, B. C. Simionescu, T. Sukhanova, M. Perminova, A. Grigoryev, G. Gubanova, and S. Bronnikov, *J. Incl. Phenom. Macrocycl. Chem*., **63**, 355 (2009).
(24) T. Girek, *J. Incl. Phenom. Macrocycl. Chem.*, **76**, 237 (2013).
(25) H. Y. Luo, Y. Liu, Z. J. Yu, S. Zhang, and B. J. Li, *Biomacromolecules*, **9**, 2573 (2008).
(26) L. Huang, E. Allen, and A. E. Tonelli, *Polymer*, **40**, 3211 (1999).
(27) P. J. Pan, W. H. Kai, B. Zhu, T. Dong, and Y. Inoue, *Macromolecules*, **40**, 6898 (2007).
(28) L. J. Liu, J. J. Du, H. Q. Dong, and L. Q. Liao, *Polym. Prepr*., **52**, 276 (2011).
(29) X. T. Shuai, F. E. Porbeni, M. Wei, T. Bullions, and A. E. Tonelli, *Macromolecules*, **35**, 3778 (2002).
(30) H. Jiao, S. H. Goh, and S. Valiyaveettil, *Macromolecules*, **34**, 8138 (2001).
(31) H. Okumura, Y. Kawaguchi, and A. Harada, *Macromolecules*, **36**, 6422 (2003).
(32) J. Lu, I. D. Shin, S. Nojima, and A. E. Tonelli, *Polymer*, **41**, 5871 (2000).
(33) W. Zhai, Y. Ko, W. Zhu, A. Wong, C. B. Park, *Int. J. Mol. Sci*., **10**, 5381 (2009).
(34) J. C. Huang, X. Li, T. T. Lin, C. B. He, K. Y. Mya, Y. Xiao, and J. Li, *J. Polym. Sci.*, *Part B: Polym. Phys.,* **42**, 1173 (2004).
(35) H. Jiao, S. H. Goh, and S. Valiyaveettil, *Macromolecules*, **35**, 1399 (2002).
(36) P. Song, G. Y. Chen, Z. Y. Wei, Y. Chang, W. X. Zhang, and J. C. Liang, *Polymer*, **53**, 4300 (2012).
(37) R. Legras, J. P. Mercier, and E. Nield, *Nature*, **304**, 432 (1983).
(38) K. A. Mauritz, E. Baer, and A. J. Hopfinger, *J. Polym. Sci. Part D: Macromol. Rev.*, **13**, 1 (1978).
(39) T. Kawai, R. Lijima, Y. Yamamoto, and T. Kimura, *Polymer*, **43**, 7301 (2002).
(40) H. G. Haubruge, R. Daussin, A. M. Jonas, R. Legras, J. C. Wittmann, and B. Lotz, *Macromolecules*, **36**, 4452 (2003).
(41) N. Jacquel, K. Tajima, N. Nakamura, H. Kawachi, P. J. Pan, and Y. Inoue, *J. Appl. Polym. Sci.*, **115**, 709 (2010).
(42) M. T. Viciosa, N. M. Alves, T. Oliveira, M. Dionísio, and J. F. Mano, *J. Phys. Chem. B*, **118**, 6972 (2014).
(43) Z. J. Yu, Y. Liu, M. M. Fan, X. W. Meng, B. J. Li, and S. Zhang, *J. Polym. Sci.*, *Part B: Polym. Phys.*, **48**, 951 (2010).
(44) A. Lendlein and R. Langer, *Science*, **296**, 1673 (2002).
(45) M. Kohl, D. Brugger, M. Ohtsuka, and T. Takagi, *Sens. Actuators A: Phys.*, **114**, 445 (2004).
(46) X. F. Zhang, H. Hua, X. Y. Shen, and Q. Yang, *Polymer*, **48**, 1005 (2007).